

Spin Liquid States in Kitaev-Heisenberg Model

Sanjib Kumar Das

*A dissertation submitted for the partial fulfilment
of BS-MS dual degree in Science*



Indian Institute of Science Education and Research Mohali
April 2017

Certificate of Examination

This is to certify that the dissertation titled **Spin Liquid States in Kitaev-Heisenberg Model** submitted by **Sanjib Kumar Das (Reg. No. MS12066)** for the partial fulfillment of BS-MS dual degree programme of the Institute, has been examined by the thesis committee duly appointed by the Institute. The committee finds the work done by the candidate satisfactory and recommends that the report be accepted.

Dr. Abhishek Chaudhuri

Dr. Yogesh Singh

Dr. Sanjeev Kumar
(Supervisor)

Dated: April 21, 2017

Declaration

The work presented in this dissertation has been carried out by me under the guidance of Dr. Sanjeev Kumar at the Indian Institute of Science Education and Research Mohali.

This work has not been submitted in part or in full for a degree, a diploma, or a fellowship to any other university or institute. Whenever contributions of others are involved, every effort is made to indicate this clearly, with due acknowledgement of collaborative research and discussions. This thesis is a bonafide record of original work done by me and all sources listed within have been detailed in the bibliography.

Sanjib Kumar Das
(Candidate)

Dated: April 21, 2017

In my capacity as the supervisor of the candidates project work, I certify that the above statements by the candidate are true to the best of my knowledge.

Dr. Sanjeev Kumar
(Supervisor)

Acknowledgments

I would first like to express my sincere gratitude to my thesis supervisor Dr. Sanjeev Kumar for guiding me in the final year thesis project. He has been really inspiring and encouraging throughout my project. He was always there to help whenever I ran into any problem. I am really thankful to him for many such valuable and insightful discussions.

I would like to thank my other thesis committee members, Dr. Abhishek Chaudhuri, and Dr. Yogesh Singh. Discussion with Dr. Abhishek Chaudhuri has been always fruitful and motivating. I would also like to thank IISER Mohali for giving me the opportunity to pursue science. IISER Mohali library is duly acknowledged for providing great facilities. I am extremely grateful to the faculties of IISER Mohali for their cooperative behaviour. I would like to take this opportunity to thank Department of Science and Technology (DST) for providing me the INSPIRE scholarship.

I am thankful to the other group members for their help. Specifically, Ayushi, Abhinay have been really helpful. I would like to thank my friends who have always supported me. Specifically, Martik, Anuj, Mushir, Anirudh, Gaurav, Vishnu, Abhijeet, Aditya, Maruthi, Shrinit, Vijith. I should also mention that I have always enjoyed the Physics discussions with Vishnu, Abhijeet, Gaurav, Pratik, Vikash and Aditya.

Finally, I am grateful to my parents who have always encouraged me to pursue my dream and supported me in all situations.

List of Figures

1.1	spin liquid[26]	3
2.1	Honeycomb lattice with three anisotropic interaction	9
2.2	Phase diagram of Kitaev model with all $u_{i,j} = 1$ sector. The bigger triangular part is $J_x + J_y + J_z = 1$. [1]	22
2.3	(2.3a) A_x gapped phase for $J_x, J_y, J_z = 0.6, 0.1, 0.3$ respectively. (2.3b) A_y gapped phase for $J_x, J_y, J_z = 0.2, 0.7, 0.1$ respectively. (2.3c) A_z gapped phase for $J_x, J_y, J_z = 0.1, 0.2, 0.7$ respectively. (2.3d) boundary of the gapped and gapless phase for $J_x(0.1) + J_y(0.4) = J_z(0.5)$	23
2.4	Mid point of the Phase B where energy vanishes.	24
2.5	Phase diagram of KH model[6].	26
3.1	(3.1a) $C_v(T, \alpha = 0)$ (3.1b) $C_v(T, \alpha = 0.5)$ (3.1c) $C_v(T, \alpha = 0.75)$ (3.1d) $C_v(T, \alpha = 1)$	29
3.2	(3.2a) $E(T, \alpha = 0)$ (3.2b) $E(T, \alpha = 0.5)$ (3.2c) $E(T, \alpha = 0.75)$ (3.2d) $E(T, \alpha = 1)$	30
3.3	(3.3a) $M(T, \alpha = 0)$ (3.3b) $M(T, \alpha = 0.5)$ (3.3c) $M(T, \alpha = 1)$	30
3.4	(3.4a) $C_v(T, \alpha = 0)$ (3.4c) $C_v(T, \alpha = 0.5)$ (3.4b) $E(T, \alpha = 0)$ (3.4d) $E(T, \alpha = 0.5)$	31
3.5	(3.4e) $C_v(T, \alpha = 1)$ (3.4f) $E(T, \alpha = 1)$	32
3.6	(3.6a) $M(T, \alpha = 0)$ (3.6b) $M(T, \alpha = 0.5)$ (3.6c) $M(T, \alpha = 1)$	32
3.7	(3.7a) Structure factor for $\alpha = 1$ on 30×30 triangular lattice. (3.7b) Structure factor for $\alpha = 0$ on 30×30 triangular lattice.	33

Abbreviations

CMC	Classical Monte-Carlo
KH	Kitaev-Heisenberg
CMFT	Cluster Mean Field Theory

Dedicated to my family

Abstract

Frustrated spin systems show exotic ground state known as spin liquid. Spin liquid is a disordered state where the system does not undergo any magnetic ordering even at very low temperature due to fluctuations. Understanding of spin liquid is challenging as it is hard to find their existence experimentally. Spin liquid can show both gapless and gapped excitations. However, spin liquid cannot be studied with conventional Landau-Ginzburg order parameter as it does not show any spontaneous symmetry breaking. Rather, the gapless phases are protected by some gauge fields. Recently, Kitaev[1] has proposed a two dimensional exactly solvable spin 1/2 model on honeycomb lattice which hosts quantum spin liquid as its ground state. This model has bond directional interactions which make it a frustrated system and it is different than geometrical frustration. This has generated significant interests to look for materials which can show Kitaev like spin interaction. Kitaev like interaction is observed in the presence of Heisenberg spin coupling term which is called Kitaev-Heisenberg model. Recently, people have found bond directional interaction in iridates[7] and observed the Kitaev spin liquid behaviour in $\alpha - RuCl_3$ [10]. In first part of my thesis work, I understood the analytical techniques required to solve the Kitaev model[1]. Using the fermionisation of spin 1/2 method, Kitaev spin 1/2 interacting Hamiltonian can be simplified to a non-interacting Majorana fermions hopping Hamiltonian in presence of constant background gauge fields. In the second part of my thesis, classical Kitaev-Heisenberg Hamiltonian[9] was explored. In order to understand classical KH model, certain thermodynamical quantities like energy, specific heat, magnetisation, have been calculated using classical Monte-Carlo simulations on honeycomb lattice and triangular lattice. We have shown that if we go away from the Kitaev limit, the system shows phase transition on honeycomb lattice. But for $\alpha = 1$ (Kitaev limit) the specific heat and energy curves show no transitions on honeycomb lattice. However, using CMC we observe that for triangular lattice, the system always shows phase transitions occurring at low temperature for all ranges of α . Corresponding structure factors plots guide us to the ferromagnetic($\alpha = 1$) and anti-ferromagnetic($\alpha = 0$) ground states on triangular lattice.

Contents

List of Figures	i
Abbreviations	iii
Abstract	vii
1 Introduction	1
1.1 Classifications of Materials and Methods	2
1.2 Spin-Liquids	3
1.3 Motivation	5
1.4 Thesis Plan	7
2 Theoretical Background	9
2.1 Kitaev model on honeycomb lattice	9
2.2 Kitaev Hamiltonian	10
2.3 Symmetries and Conserved quantities	11
2.4 Fermionisation Technique for Spin 1/2	12
2.5 Diagonalising the Fermionised Hamiltonian	18
2.6 Excitation and Phase Diagram of Kitaev Model	20
2.7 Dispersion plots for various phases	23
2.8 Kitaev-Heisenberg Model	25
2.9 KH Hamiltonian and its Phase Diagram	25
3 Results and Discussion	27
3.1 Classical KH Hamiltonian	27
3.2 Metropolis Algorithm	27
3.3 Thermodynamical Quantities	28
3.4 MC results on honeycomb lattice	28
3.5 MC results on triangular lattice	31

3.6	Structure Factor	33
3.7	Conclusion	34
3.8	Future Outlook	35
A	Anti-Commutation Relation	37
	Bibliography	

Chapter 1

Introduction

Real materials around us are diverse. Understanding the nature of real materials is challenging as they show various exotic phases. Condensed Matter Physics tries to capture the understanding of these real materials by modelling them using various effective methods theoretically and experimentally. As the number of real materials are huge, we expect to discover plenty of exotic characters shown by them. It is this existence of various exotic phases which makes this field interesting as well as challenging. Every kind of material should be modelled appropriately so that we can understand its properties and behaviours completely.

Towards the understanding of such materials, we look for suitable model to describe them separately. For example, Free Electron model is one of the simplest models which can describe the properties of metals like Na, K in a very accurate sense. One of the very interesting models which describes the properties of transition metals is Tight Binding model.

But all these models do not incorporate electron-electron interaction. However, in real materials electron-electron interaction is present. If we take into account electron-electron interaction in the model Hamiltonian, it gets incredibly difficult to solve them analytically. For instance, Hubbard model which is one of the simplest toy models which includes electron-electron interaction is still unsolved even in two dimension analytically. So, there are very few models which can be exactly solved in Condensed Matter Physics if we incorporate electron electron interaction. For this purpose, we are limited to the analytical tools available to us and it is fruitful to explore models with the help of computer simulation.

Using computer simulations we can probe the systems at any scale and calculate quantities we are interested in. In addition to that, One can also predict the emergence of new phases of matter with the help of simulations.

1.1 Classifications of Materials and Methods

The real materials more or less can be categorised them in the following list;

- Metals
- Insulators
- Semi-Conductors
- Semi-metals
- Mott Insulators
- Topological Insulators
- Superconductors
- Magnets
- Spin-Liquids

The research in Condensed Matter Physics is developing rapidly everyday and this list will require new additions to classify new kind of systems in future. There are several computational techniques that have also been developed to investigate real materials. Some of them which are commonly used are following;

- Exact Diagonalisation
- Classical Monte-Carlo
- Quantum Monte Carlo
- Hatree-Fock and Density Functional Method
- Density Matrix Renormalisation Group Method
- Cluster Mean Field Theory Method

1.2 Spin-Liquids

In Condensed Matter systems most common phases are liquid, solid and gas. Any of such phases can be characterised by some local order parameter. This order parameters take different values in different phases. As there exists symmetry in phases one can define such order parameters corresponding to particular phase. When the symmetry is broken spontaneously we can have phase transition. It means that we can go from one phase to another phase.

Similar analog can be drawn to magnetism. Magnetism occurs due to the electron-

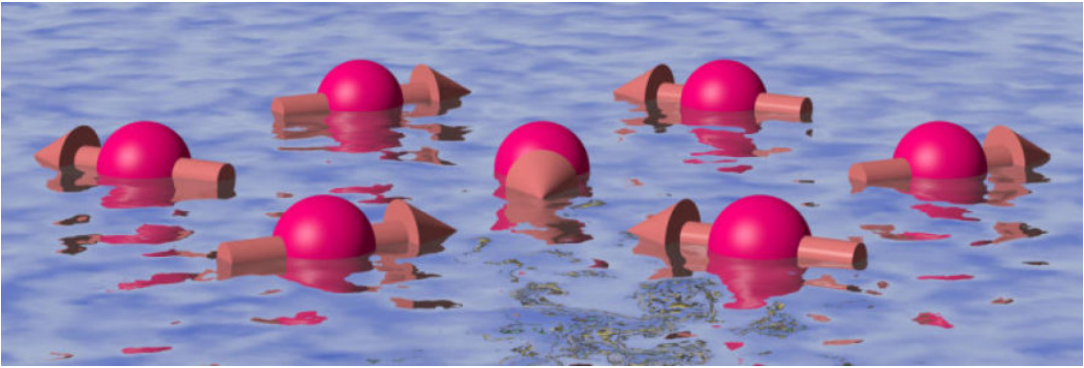


Figure 1.1: spin liquid[26]

electron interaction in the system. It can be understood by studying various spin models. Ising model, Hubbard model, Heisenberg model are some of the key models to understand magnetism. Solid phases of matter can be thought of as the ordered Ferromagnetic or Anti-ferromagnetic states in magnetism. Gas phase could be associated with Paramagnetism where spins are not ordered in arranged manners. It is interesting that the liquid phase of matter does not have any counterpart in magnetism. To establish such an analogy of liquid state in magnetism we have Spin Liquid. Spin liquid is a disordered phase of matter in which fluctuations dominate even at temperature close to 0 K. Generally, when we cool down the system, system goes to some ordered state. But for spin liquids due to the presence of large degeneracy in ground states, the system fluctuates even at low temperature. Spin liquid is a signature of frustrated spin system[23].

For instance, a triangular lattice which has anti-ferromagnetic interaction term among spins is a frustrated spin system as the third spin will try to satisfy the need of other two spins simultaneously. This competition to satisfy the overall nature of anti-ferromagnetic interaction makes the system frustrated. We can realise that in order for the system to be anti-ferromagnetic in nature, the system can have six fold degeneracy. This large degeneracy of the system gives rise to spin liquid type ground state to appear where there is no ordering. Nevertheless, this frustration is arising due to the geometry of the lattice. This is called geometrical frustration.

The concept of quantum spin liquid was first proposed by Anderson in 1973. Since then, the quest for experimental realisation of spin liquid is on. More detail about spin liquids can be found in this review article[16]. Some systems which have been experimentally discovered to host quantum spin liquid ground state are following:

- Two dimensional triangular lattice: $k-(BEDT-TTF)_2Cu_2(CN)_3$, $Ba_3IrTi_2O_9$.
- Two dimensional Kagome lattice: $ZnCu_3(OH)_6Cl_2$ (Herbertsmithite).
- Two dimensional honeycomb lattice: $\alpha - RuCl_3$, A_2IrO_3 where ($A = Na, Li$).

To capture spin liquid like character in experiments is very much challenging due to their fluctuations. Frustrated systems can be characterised by a parameter called frustration parameter which is defined by the following way:

$$f = \frac{|\Theta_{CW}|}{T_c} \quad (1.1)$$

where Θ_{CW} is the Curie-Weiss temperature and T_c is the transition temperature. For frustrated systems $f \gg 1$. in the case of frustrated systems even at very low temperature, there does not exist any long range order. Spin liquid has one more interesting property which is called fractional excitations. It is a very counter-intuitive phenomena where an electron can actually get split and show its spin, charge and orbital components independently. By performing neutron scattering experiments fractional excitations have recently been found in kagome-lattice anti-ferromagnet[3].

Interestingly, spin liquids show both gapless and gapped excitations. Gapless excitations are traditionally understood from the Goldstone mode concept where they appear due to spontaneous symmetry breaking of the system. However, in the case of spin liquids, this is not applicable as the system does not show any spontaneous symmetry breaking. For spin liquids the gapless modes are protected by gauge fields[14]. In order to understand quantum spin liquids microscopically, one can use Schwinger-boson or Schwinger-fermion techniques where spin operators are represented by either bosons or fermions. To obtain the ground state of spin liquid system, first we need to calculate the mean field ground state using Schwinger-boson or Schwinger-fermion methods. After that one can apply corresponding projection group to obtain the exact ground state of the system[13].

1.3 Motivation

Very recently, Kitaev has given an exactly solvable spin 1/2 model on two dimensional honeycomb lattice with bond directional interaction[1]. The spin component of one spin will interact with the same component of the nearest neighbour spin through the assigned bond. Hence, the model is an example of a frustrated system as at any site one spin cannot satisfy all three interaction of spin components with three other spins simultaneously. This frustration is arising from the anisotropic nearest neighbour interaction which is different than geometrical frustration. The ground state of this model is a quantum spin liquid which can show gapless and gapped excitations. To characterise the nature of spin liquid theoretically, quasi-particle fractional statistics are needed. In two dimension spin liquid can give rise to excitations of quasi-particles which are called Anyons. Anyons are neither Bosons nor Fermions. They follow a different statistics called Braid group. Kitaev model shows both type of spin liquids:

- Gapped phase spin liquid
- Gapless \mathbb{Z}_2 spin liquid

The gapless \mathbb{Z}_2 spin liquid supports fractionalised excitations. Majorana fermions could be observed here as quasi-particles. These particles are called non-abelian anyons. The gapped phase supports abelian anyon excitation.

Recently, people are trying to understand finite temperature properties of Kitaev model[20]. In doing so, one needs to understand the dynamics of Majorana fermions. Here, Majorana fermions can be divided into two categories. One is localised and the other is itinerant. The specific heat has two peaks meaning there is a crossover between this two different temperature phases. The high temperature phase is the contribution of itinerant Majorana fermions where as the low temperature region is caused due to the thermal fluctuations of localised Majorana fermions. While calculating thermodynamical quantities, the value of all background gauge fields are set to some constant. So, one can derive the dispersion relation and density of states of Majorana fermions for certain configuration of background gauge fields. This gives a nice way to understand the behaviours of Majorana fermions.

Experimental realisation of Kitaev like interaction in real materials is challenging. However, in presence of Heisenberg exchange term, Kitaev like interaction can be explored. The presence of Heisenberg spin exchange term brings magnetic ordering at low temperature.

Transition metal oxides with partially filled $4d$ or $5d$ orbitals show strong spin-orbit coupling which can exhibit unconventional magnetic ordering. Materials with strong-orbit coupling can also show anisotropic interaction. In Na_2IrO_3 material, Ir^{4+} ions are in $5d^5$ configuration forming two dimensional hexagonal layers. in presence of octahedral crystal field there is a splitting in orbitals into t_{2g} and e_g . Then due to strong spin orbit coupling t_{2g} level is filled with $j = 3/2$ and e_g is partially filled with $j = 1/2$ band. The behavior of this effective $j = 1/2$ moment can be described by KH model. A coherent description of different kinds of Kitaev material can be found in the article[17]. So, KH model on iridate materials is a very interesting model to explore spin liquid state along with some long range magnetic ordered states. Recently, people are also exploring KH model on triangular lattice[19].

1.4 Thesis Plan

Motivated by the exotic features of frustrated spin system, the work has been carried out to understand spin liquids. The work can be divided into two parts:

- Understanding the exact analytical solution of Kitaev model and theoretical understanding of spin liquids.
- Numerical investigations of classical KH model on honeycomb lattice and triangular lattice using Classical Monte-Carlo method.

Chapter 2

Theoretical Background

In this chapter I will focus on the exact solution of the Kitaev model. In doing so, I will discuss about some symmetries and corresponding conserved quantities which will divide the dimension of the original Hilbert space into two sectors. After which, I will go through the technique called fermionisation of spin $1/2$ and diagonalise the Hamiltonian to get the energy spectrum. The phase diagram of Kitaev model will be explained. Finally, I will briefly introduce the Kitaev-Heisenberg model and its Phase diagram which have been there in the literature.

2.1 Kitaev model on honeycomb lattice

Kitaev model on honeycomb lattice is a two dimensional exactly solvable spin $1/2$ model. This model captures the physics of strongly correlated electrons. It is a very interesting model which supports fractional excitations. The Kitaev model described on honeycomb lattice looks like following:

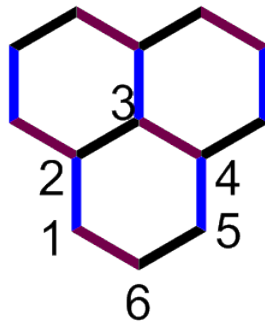


Figure 2.1: Honeycomb lattice with three anisotropic interaction

The model describes the interaction between spin 1/2 which are residing at each site of the hexagon. The bonds shown by different colors represent anisotropic interaction between the spins. Thus we need to label the links properly. The black color link represents 'x' bond, violet color link represents 'y' bond and the blue color link represents the 'z' bond. We have labeled the bonds x,y,z because any two nearest neighbour spins will interact with their spin components corresponding to the assigned link. If a spin is connected to its neighbour by x bond then their x component of spin will only interact. So is true for the other bonds.

It is in this sense the system has anisotropic interaction. Each spin at one site cannot satisfy its interaction of all three spin components with nearest neighbour spin. That is why this system is a frustrated spin system. It is important to mention that this frustration is different from geometrical frustration where frustration appears due to the geometrical structure of lattice. For example, a spin system on triangular lattice which has anti-ferromagnetic ground state will show geometrical frustration. Frustrated systems show very interesting features. One of which is the presence of spin liquid ground state. This kind of systems do not show any magnetic ordering even at very low temperature i.e. fluctuation still dominates even at low temperature which prevents the system from ordering.

2.2 Kitaev Hamiltonian

The Hamiltonian[1] of the system can be written as following:

$$H = -J_x \sum_{\langle ij \rangle, x} \sigma_i^x \sigma_j^x - J_y \sum_{\langle ij \rangle, y} \sigma_i^y \sigma_j^y - J_z \sum_{\langle ij \rangle, z} \sigma_i^z \sigma_j^z \quad (2.1)$$

where the summation is taken over all nearest neighbour spins i and j and all the links. $\sigma^x, \sigma^y, \sigma^z$ are the Pauli spin 1/2 matrices. J_x, J_y, J_z are the exchange constants. So, we need to solve the Hamiltonian in order to get the energy spectrum of the system.

We know that if we find some symmetries of the system then it will correspond to some conserved quantities. Hence, it can reduce the large dimension of the Hilbert space of the system. So, it is therefore important to investigate for symmetries before diagonalising the Hamiltonian.

2.3 Symmetries and Conserved quantities

In order to find symmetries of the system we focus on each plaquette. On each plaquette we can define one operator W_p in the following form;

$$W_p = \sigma_1^x \sigma_2^y \sigma_3^z \sigma_4^x \sigma_5^y \sigma_6^z \quad (2.2)$$

We can easily identify how the above form of the operator is obtained. We consider one plaquette and write down all possible link from the Fig.(2.1).

$$W_p = \sigma_1^z \sigma_2^z \sigma_2^x \sigma_3^x \sigma_3^y \sigma_4^y \sigma_4^z \sigma_5^z \sigma_5^x \sigma_6^x \sigma_6^y \sigma_1^y \quad (2.3)$$

Now if we use the relation $\sigma^x \sigma^y = i \epsilon^{xyz} \sigma^z$ then W_p retains the form (2.2).

The operator W_p remarkably commutes with the Hamiltonian of the system H giving rise to some local conserved quantities.

First we define the following relations:

$$\{\sigma_{i\alpha}, \sigma_{i\beta}\} = 2\delta_{\alpha\beta} \quad \text{where} \quad \alpha, \beta = x, y, z \quad (2.4)$$

$$[\sigma_{i\alpha}, \sigma_{j\beta}] = 0 \quad \text{if} \quad i \neq j \quad (2.5)$$

The above two relations indicate that all components of spins on various links are mutually commuting where as on a given link different Cartesian spin components anti-commute.

Let us take only one component of the Hamiltonian, say z component of spin interaction term and check the commutation relation with the operator W_p .

$$[W_p, \sigma_1^z \sigma_2^z] = \sigma_1^x \sigma_2^y \sigma_3^z \sigma_4^x \sigma_5^y \sigma_6^z \sigma_1^z \sigma_2^z - \sigma_1^z \sigma_2^z \sigma_1^y \sigma_2^x \sigma_3^z \sigma_4^x \sigma_5^y \sigma_6^z \quad (2.6)$$

By using the above two commutation relations, we can bring $\sigma_1^z \sigma_2^z$ to the left in the first term and it will then cancel out with the other term. Hence

$$[W_p, \sigma_1^z \sigma_2^z] = 0 \quad (2.7)$$

Similarly y component interaction and z component interaction term of the Hamiltonian will commute with the operator W_p .

Thus, the operator W_p commutes with the total Hamiltonian H .

$$[W_p, H] = 0 \quad (2.8)$$

It means on each plaquette there is a conserved quantity which is associated with this operator W_p . So, the operator W_p and H will have same set of eigenfunction. One more important thing is to notice the structure of the operator W_p . The structure can easily guide us to get what is the corresponding eigenvalues of the operator W_p . We can take the square of W_p and see its form which is the following;

$$W_p^2 = (\sigma_1^x \sigma_2^y \sigma_3^z \sigma_4^x \sigma_5^y \sigma_6^z) (\sigma_1^x \sigma_2^y \sigma_3^z \sigma_4^x \sigma_5^y \sigma_6^z) \quad (2.9)$$

We can pair all the σ^x , σ^y and σ^z operator together and using the identity form of σ^2 operator we see that,

$$W_p^2 = 1 \quad (2.10)$$

$$W_p = +1, -1 \quad (2.11)$$

Hence, the operator W_p has two eigenvalues $+1$ or -1 . So, can divide the Hilbert space of the system into two sectors. One sector corresponds to the eigenvalue $W_p = 1$ and the other sector corresponds to $W_p = -1$. Initially the dimension of the Hilbert space was 2^n where n is the number of spins present in the system. The degrees of freedom described by $\{W_p\}$ will be equal to the number of plaquettes $n/2$. Thus, each of this sectors will correspond to the Hilbert space which is of $2^{n/2}$ dimensional.

The variables W_p act like a static \mathbb{Z}_2 Ising field. So, the problem boils down to solve the Hamiltonian for each such configuration of W_p which can have two values 0 or 1 .

2.4 Fermionisation Technique for Spin 1/2

In this section we will understand how the problem of interacting spin $1/2$ can be mapped to non interacting Majorana fermions. To solve the Hamiltonian we need to use the technique called fermionisation[1] of spin $1/2$ where each complex Dirac fermion is represented by two real Majorana fermions.

First, we are defining the system with two spin $1/2$ present at each vertex of the hexagon. So, we need to introduce four Majorana fermions for two Dirac fermions present at each vertex.

The creation and annihilation operators for this two Dirac fermions are $C_1^\dagger, C_2^\dagger, C_1, C_2$. The corresponding four Majorana operators are the following:

$$C = (C_1 + C_1^\dagger) \quad (2.12)$$

$$C^x = (1/i)(C_1 - C_1^\dagger) \quad (2.13)$$

$$C^y = (C_2 + C_2^\dagger) \quad (2.14)$$

$$C^z = (1/i)(C_2 - C_2^\dagger) \quad (2.15)$$

Where all the Majorana fermionic operators obey the anti-commutation relation:

$$\{C^\alpha, C^\beta\} = 2\delta_{\alpha\beta} \quad \text{where} \quad \alpha, \beta = x, y, z \quad (2.16)$$

$$C^\alpha = C^{\alpha\dagger} \quad (2.17)$$

$$C^\beta = C^{\beta\dagger} \quad (2.18)$$

In the above anti-commutation relation the site index has not been introduced for the Majorana operators as they are living on the same site. Nevertheless, all the Majorana operators which are at different site will commute with each others. The equations (2.17) and (2.18) are true because Majorana particles are their own antiparticle.

Now we can represent the spin 1/2 operators in the Hamiltonian with these new four Majorana fermionic operators.

$$\sigma^x = iC^x C \quad (2.19)$$

$$\sigma^y = iC^y C \quad (2.20)$$

$$\sigma^z = iC^z C \quad (2.21)$$

With this construction one can easily check that the spin 1/2 operators follow the fermionic anti-commutation relation for $\alpha \neq \beta$ (A.1). In order to satisfy Pauli spin algebra there is one more condition which needs to be satisfied by these Majorana fermionic operators.

$$\sigma^x \sigma^y \sigma^z = i \quad (2.22)$$

We can multiply (2.19), (2.20), (2.21) and the resulting expression is

$$\sigma^x \sigma^y \sigma^z = iC^x C^y C^z C \quad (2.23)$$

One has to put a constraint on Majorana operators to satisfy the expression (2.22).

The constraint is $C^x C^y C^z C = 1$. We call $C^x C^y C^z C$ a new operator \hat{D} . This new operator can be expressed as following (A.2) in terms of spin 1/2 operators.

$$\hat{D} = (2C_1^\dagger C_1 - 1)(2C_2^\dagger C_2 - 1) \quad (2.24)$$

\hat{D} should have the eigen value 1 which came from applying the constraint. Earlier, we mentioned that at each site we have two spin 1/2. So, the Fock space is four dimensional. The states can be represented with the occupation number notation as $|0,0\rangle$, $|0,1\rangle$, $|1,0\rangle$, $|1,1\rangle$. Acting the operator \hat{D} on these states should give the eigenvalue 1.

$$\begin{aligned} \hat{D}|0,0\rangle &= (2C_1^\dagger C_1 - 1)(2C_2^\dagger C_2 - 1)|0,0\rangle \\ &= (4C_1^\dagger C_1 C_2^\dagger C_2 - 2C_1^\dagger C_1 - 2C_2^\dagger C_2 + 1)|0,0\rangle \\ &= -4C_1^\dagger C_2^\dagger C_1 C_2 |0,0\rangle - 2C_1^\dagger C_1 |0,0\rangle - 2C_2^\dagger C_2 |0,0\rangle + 1|0,0\rangle \\ &= 1|0,0\rangle \end{aligned}$$

The first three terms give 0 as the rightmost annihilation operator destroys the state. So, we see that the operator retains its eigenvalue 1.

$$\begin{aligned} \hat{D}|1,0\rangle &= (2C_1^\dagger C_1 - 1)(2C_2^\dagger C_2 - 1)|1,0\rangle \\ &= (4C_1^\dagger C_1 C_2^\dagger C_2 - 2C_1^\dagger C_1 - 2C_2^\dagger C_2 + 1)|1,0\rangle \\ &= -4C_1^\dagger C_2^\dagger C_1 C_2 |1,0\rangle - 2C_1^\dagger C_1 |1,0\rangle - 2C_2^\dagger C_2 |1,0\rangle + 1|1,0\rangle \\ &= (0 - 2 + 0 + 1)|1,0\rangle \\ &= -1|1,0\rangle \end{aligned}$$

Here we see that the eigenvalue of the operator \hat{D} is -1 which is not expected as it will violate Pauli's spin algebra. Similarly, if we operate \hat{D} on the state $|0,1\rangle$ it will give the eigenvalue -1 where as the state $|1,1\rangle$ will give the correct eigenvalue of 1. We can clearly infer from the above calculation that the states which gave eigenvalue -1 are unphysical. If we want to retain all the possible physical states in the Hilbert space then we have to get rid of these unphysical states. Here in these case the physical states are $|0,0\rangle$ and $|1,1\rangle$. And the corresponding unphysical states are $|0,1\rangle$ and $|1,0\rangle$.

Our next task is to eliminate all these unphysical states from the Hilbert space. In order to project out all the unphysical states we can construct one operator for each site i

$$\hat{P}_i = \frac{1 + \hat{D}_i}{2} \quad (2.25)$$

If we operate this $\hat{P}[1]$ on the states $|0, 1\rangle$ and $|1, 0\rangle$ it will project out these two states from the Hilbert space.

$$\begin{aligned} \hat{P}|0, 1\rangle &= \frac{1 + \hat{D}_i}{2}|0, 1\rangle \\ &= \frac{1}{2}|0, 1\rangle + \frac{1}{2}(2C_1^\dagger C_1 - 1)(2C_2^\dagger C_2 - 1)|0, 1\rangle \\ &= \frac{1}{2}|0, 1\rangle + \frac{1}{2}(-1|0, 1\rangle) \\ &= 0 \end{aligned} \quad (2.26)$$

Similarly, $\hat{P}|1, 0\rangle = 0$ is also true. So, the projection operator \hat{P} is able to project out all the unphysical states from the Hilbert space. Though we can define such an operator for each site, the process of eliminating all the unphysical states is cumbersome. So, if we are interested in finding out the eigen states of the system systematically then we should use another method called Jordan-Wigner transformation[24].

One should notice why these unphysical states appear in the Hilbert space. The reason for this is when we are introducing the Majorana fermionic operators for the spin 1/2, we are enlarging the corresponding Hilbert space with many gauge copies. These extra states are present in the Hilbert space but are not significant. The spectrum of the Hamiltonian will be same even in the extended Hilbert space as we can verify that when we take the commutator of \hat{D}_i and H .

$$\begin{aligned} [D_i, \sigma_i^x] &= i \{C^x C^y C^z C C^x C - C^x C C^x C^y C^z C\} \\ &= i \{-C^x C^x C^y C^z C^2 + C^x C^2 C^x C^y C^z\} \\ &= i \{C^y C^z - C^y C^z\} \\ &= 0 \end{aligned} \quad (2.27)$$

The expression (2.27) is obtained using the anti-commutation relations of Majorana fermionic operators which give $C^2 = 0, (C^x)^2 = 0$. We took the commutator of \hat{D}_i and σ_i^x because σ_j^x will anyway commute with \hat{D}_i (because spin components at different site always commute).

We can carry out the same thing and observe that all three terms in the Hamiltonian commute with the operator \hat{D}_i and hence the spectrum of the Hamiltonian retains same in the extended Hilbert space also. Thus, we need to diagonalise this fermionised Hamiltonian to get the energy spectrum.

Now let us write down the Hamiltonian in terms of Majorana fermionic operators:

$$\begin{aligned} H &= -J_x \sum_{\langle ij \rangle, x} (i)^2 C_i^x C_i C_j^x C_j - J_y \sum_{\langle ij \rangle, y} (i)^2 C_i^y C_i C_j^y C_j - J_z \sum_{\langle ij \rangle, z} (i)^2 C_i^z C_i C_j^z C_j \\ &= -J_x \sum_{\langle ij \rangle, x} (i C_i^x C_j^x)(-i C_i C_j) - J_y \sum_{\langle ij \rangle, y} (i C_i^y C_j^y)(-i C_i C_j) - J_z \sum_{\langle ij \rangle, z} (i C_i^z C_j^z)(-i C_i C_j) \end{aligned}$$

$$\boxed{H = J_x \sum_{\langle ij \rangle, x} (i C_i^x C_j^x)(i C_i C_j) + J_y \sum_{\langle ij \rangle, y} (i C_i^y C_j^y)(i C_i C_j) + J_z \sum_{\langle ij \rangle, z} (i C_i^z C_j^z)(i C_i C_j)} \quad (2.28)$$

It is clear that the Hamiltonian [22] described by the equation (2.28) is quartic in Majorana fermionic operators. The terms $(i C_i^x C_j^x)$, $(i C_i^y C_j^y)$, $(i C_i^z C_j^z)$ individually commute with the Hamiltonian and hence correspond to conserved quantities. We can denote them with a new notation which is the following:

$$i C_i^x C_j^x = u_{i,j}^x \quad (2.29)$$

$$i C_i^y C_j^y = u_{i,j}^y \quad (2.30)$$

$$i C_i^z C_j^z = u_{i,j}^z \quad (2.31)$$

As these quantities (2.29), (2.30), (2.31) are conserved, we can take them to be some constant gauge fields and then the Hamiltonian reduces to quadratic in nature. These quantities are some constant fields which are sitting on x, y and z bonds. If we replace these quantities and rewrite the Hamiltonian, it will look like:

$$\boxed{H = J_x \sum_{\langle ij \rangle, x} u_{i,j}^x (i C_i C_j) + J_y \sum_{\langle ij \rangle, y} u_{i,j}^y (i C_i C_j) + J_z \sum_{\langle ij \rangle, z} u_{i,j}^z (i C_i C_j)} \quad (2.32)$$

The above Hamiltonian describes the tight binding Majorana fermions hopping in presence of constant \mathbb{Z}_2 gauge fields defined on each x, y and z bonds.

One can ask what are the these constant values which can be taken by these constant fields. For that we have to notice the structure of $u_{i,j}^\alpha$ where $\alpha = x, y, z$. It is easy to realize that $|u_{i,j}|^2 = 1$. Hence the eigen values of $u_{i,j}$ are $+1$ or -1 . Thus we can solve the Hamiltonian for $+1$ or -1 configuration of $u_{i,j}$.

So after fermionisation the Hamiltonian we are getting some conserved quantities in the extended Hilbert space which are the above mentioned gauge fields. For a specific plaquette we can define one vortex operator;

$$\hat{V}_p = \prod_{\langle i,j \rangle (\text{plaquette boundary})} u_{i,j} \quad (2.33)$$

where i, j belong to different sub-lattice of the hexagon. This vortex operator should reduce to \hat{W}_p when we restrict it to the physical space where $\hat{D} = 1$. Another important thing to remember is $\hat{u}_{i,j} = -\hat{u}_{j,i}$.

$$\begin{aligned} \hat{V}_p &= \hat{u}_{2,1} \hat{u}_{2,3} \hat{u}_{4,3} \hat{u}_{4,5} \hat{u}_{6,5} \hat{u}_{6,1} \\ &= (i)^6 (-1) C_1^z C_2^z C_2^x C_3^x (-1) C_3^y C_4^y C_4^z C_5^z (-1) C_5^x C_6^x C_6^y C_1^y \\ &= \sigma_1^x \hat{D}_1 \sigma_2^y \hat{D}_2 \sigma_3^z \hat{D}_3 \sigma_4^x \hat{D}_4 \sigma_5^y \hat{D}_5 \sigma_6^z \hat{D}_6 \\ &= \sigma_1^x \sigma_2^y \sigma_3^z \sigma_4^x \sigma_5^y \sigma_6^z \end{aligned} \quad (2.34)$$

using $iC_i^z C_i^x = -\sigma_i^y D_i$ and cyclic permutation, we have got the final expression (2.34) which is same as equation (2.2). So, we can say that each of the $\hat{u}_{i,j}$ is not gauge invariant but their product over one plaquette is gauge invariant which commutes with the original Hamiltonian. Hence in the physical space where $\hat{D} = 1$ the operator $\hat{V}_p = \hat{W}_p$.

We have come close to diagonalise the Hamiltonian for certain configuration of $u_{i,j}$ and get the eigen value spectrum. However, with this technique it is tedious to get the eigen states as we need to project out all the unphysical states first. The following formula can be used to get the physical eigen state of the system:

$$|\psi\rangle_{phys} = \prod_i \left(\frac{1 + D_i}{2} \right) |\psi\rangle \quad (2.35)$$

Now, the question is for what value of the plaquette operator W_p the system corresponds to the ground state?

A proof given by Lieb[21] which states that, in order to find the minimum energy configuration one needs to take $W_p = 1$ for each plaquette which is achieved by fixing the $u_{i,j} = 1$ for every link.

2.5 Diagonalising the Fermionised Hamiltonian

We are now in the perfect position for diagonalising this fermionised Hamiltonian in presence of the constant background fields. The Hamiltonian is quadratic in Majorana operators representing a simple tight binding model. We have translational invariance symmetry in the system. So, the way to solve the Hamiltonian is to represent all the Majorana operators in the Fourier space as we do it for any general tight binding model. Honeycomb lattice is not a Bravais lattice. In order make it a Bravais lattice we can redefine a unit cell. We represent a z-link as the new unit cell and then it will get reduced to a square lattice.

$$C_i^{a,b} = \sum_k \frac{1}{\sqrt{N}} e^{i\vec{k}\cdot\vec{r}_i} C_k^{a,b} \quad (2.36)$$

where N is the number of unit cells. As it is a square lattice now, its momentum belongs to $-\pi, +\pi$. The property $C_i^\dagger = C_i$ for Majorana fermions gives one condition which is:

$$C_k = C_{-k}^\dagger \quad (2.37)$$

So, there is an inversion symmetry exists in the momentum space. Now, the two vectors which define the lattice are:

$$\hat{n}_1 = \frac{1}{2}\hat{e}_x + \frac{\sqrt{3}}{2}\hat{e}_y \quad (2.38)$$

$$\hat{n}_2 = -\frac{1}{2}\hat{e}_x + \frac{\sqrt{3}}{2}\hat{e}_y \quad (2.39)$$

Only the nearest neighbour interaction is included. After Fourier transformation and applying summation we can get the following Hamiltonian:

$$H = \sum_{k \in \frac{1}{2}B.Z} (C_{k,a}^\dagger C_{k,b}^\dagger) \begin{bmatrix} 0 & if^*(k) \\ -if(k) & 0 \end{bmatrix} \begin{pmatrix} C_{k,a} \\ C_{k,b} \end{pmatrix} \quad (2.40)$$

where

$$f(k) = (e^{-ik_x} J_x + e^{-ik_y} J_y + J_z) \quad (2.41)$$

equation (2.41) has the property of $f^*(k) = f(-k)$. The fact that the system has inversion symmetry in momentum space makes the summation go over half Brillouin zone. It is now easy to diagonalise the matrix in equation (2.40) and the corresponding eigenvalues are $\pm|f(k)|$.

In doing the diagonalisation the unitary transformation chosen is given below:

$$\begin{pmatrix} C_{k,a} \\ C_{k,b} \end{pmatrix} = \frac{1}{\sqrt{2}} \begin{bmatrix} \frac{if_k^*}{|f(k)|} & -\frac{if_k^*}{|f(k)|} \\ 1 & 1 \end{bmatrix} \begin{pmatrix} \omega_k \\ \gamma_k \end{pmatrix} \quad (2.42)$$

After diagonalising the Hamiltonian, it takes the following form;

$$H = \sum_k |f(k)| (\omega_k^\dagger \omega - \gamma_k^\dagger \gamma) \quad (2.43)$$

Here ω, γ are the quasi-particle operators. From the expression it is obvious that the minimum energy state can be obtained by filling up the quasi-particle γ_k . Hence the ground state is

$$|G.S\rangle = \prod_{k \in \frac{1}{2}B.Z} \gamma_k^\dagger |0\rangle \quad (2.44)$$

where $|0\rangle$ represents the vacuum of quasi-particle. However, this ground state is not the exact physical ground state of the system as we have solved the system with Majorana fermionic operators. And there are still unphysical states present in the enlarged Hilbert space. To obtain the exact ground state, we need to symmetrise the above ground state with the projection operator.

2.6 Excitation and Phase Diagram of Kitaev Model

The next interesting question is to ask what is the nature of excitation in the energy spectrum?

To understand the nature of the excitation we have to look whether the spectrum is gapless or gapped. So, the problem is to look for the solution of $|f(k)| = 0$. So basically, we need to solve:

$$e^{-ik_x} J_x + e^{-ik_y} J_y + J_z = 0 \quad (2.45)$$

We can separate the real and the imaginary part and then equate them to 0.

$$J_x \cos(k_x) + J_y \cos(k_y) + J_z = 0 \quad (2.46)$$

$$-J_x \sin(k_x) - J_y \sin(k_y) = 0 \quad (2.47)$$

For analysis purpose, we impose the condition that all exchange constants to be positive. Also if we take the following conditions $k_x \leq 0$ and $k_y \geq 0$ or $k_x \geq 0$ and $k_y \leq 0$ to be true then from the equation (2.47) we will get:

$$J_x \sin(k_x) = J_y \sqrt{1 - \cos^2(k_y)} \quad (2.48)$$

On squaring the above equation we get

$$J_y^2 \cos^2(k_y) = J_y^2 - J_x^2 \sin^2(k_x) \quad (2.49)$$

From equation (2.46) we have,

$$J_y \cos(k_y) = -J_x \cos(k_x) - J_z \quad (2.50)$$

Squaring the above expression we get,

$$J_y^2 \cos^2(k_y) = J_x^2 \cos^2(k_x) + J_z^2 + 2J_x J_z \cos(k_x) \quad (2.51)$$

From equation (2.49) and (2.51) we will get the following:

$$\begin{aligned}
J_x^2 \cos^2(k_x) + J_z^2 + 2J_x J_z \cos(k_x) &= J_y^2 - J_x^2 \sin^2(k_x) \\
J_x^2 \cos^2(k_x) + J_z^2 + 2J_x J_z \cos(k_x) &= J_y^2 - J_x^2 (1 - \cos^2(k_x)) \\
2J_x J_z \cos(k_x) &= J_y^2 - J_x^2 - J_z^2 \\
\cos(k_x) &= \frac{J_y^2 - J_x^2 - J_z^2}{2J_x J_z}
\end{aligned} \tag{2.52}$$

Similarly we will obtain;

$$\cos(k_y) = \frac{J_x^2 - J_y^2 - J_z^2}{2J_y J_z} \tag{2.53}$$

After all, we are looking for the values of k_x and k_y for which the energy spectrum is gapless. And the solutions for them are the following:

$$k_x = \pm \arccos \frac{J_y^2 - J_x^2 - J_z^2}{2J_x J_z} \tag{2.54}$$

$$k_y = \pm \arccos \frac{J_x^2 - J_y^2 - J_z^2}{2J_y J_z} \tag{2.55}$$

From the above two equation, we can have limitations on the exchange constants.

$$-2J_x J_z \leq J_y^2 - J_x^2 - J_z^2 \leq 2J_x J_z \tag{2.56}$$

$$-2J_y J_z \leq J_x^2 - J_y^2 - J_z^2 \leq 2J_y J_z \tag{2.57}$$

On simplifying (2.56) further we can get,

$$\begin{aligned}
J_y^2 - J_x^2 - J_z^2 &\leq 2J_x J_z \\
J_y^2 &\leq (J_x + J_z)^2 \\
\boxed{J_y} &\leq (J_x + J_z)
\end{aligned} \tag{2.58}$$

Similarly, from (2.57) we get,

$$\boxed{J_x} \leq (J_y + J_z) \tag{2.59}$$

$$-2J_x J_z \leq J_y^2 - J_x^2 - J_z^2 \tag{2.60}$$

$$-2J_y J_z \leq J_x^2 - J_y^2 - J_z^2 \tag{2.61}$$

Finally, adding the two equations above we find the last inequality:

$$\boxed{J_z \leq (J_x + J_y)} \quad (2.62)$$

Thus, we see that the spectrum will be gapless if all the three inequalities (2.58), (2.59) and (2.62) are satisfied simultaneously. These three inequalities are called triangle inequalities. If one of these inequalities is even violated, the system will not show gapless excitation. Having been equipped with all the information, we can now look at the phase diagram.

If we restrict the plane by the $J_x + J_y + J_z = 1$. The phase diagram of Kitaev model will look like:

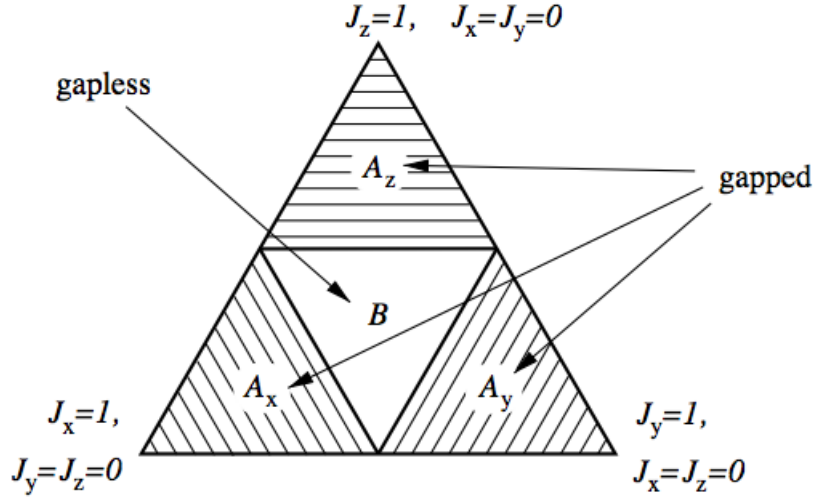


Figure 2.2: Phase diagram of Kitaev model with all $u_{i,j} = 1$ sector. The bigger triangular part is $J_x + J_y + J_z = 1$. [1]

In Fig.(2.2) the phase B is the gapless phase where all three triangle inequalities hold. The other three phases A_x , A_y , and A_z are the gapped ones where the inequalities violate. Depending on the various values of exchange constants, the corresponding phases are decided.

2.7 Dispersion plots for various phases

In this section, we will plot the dispersion relation for the four phases of Kitaev model. The expression (2.41) will be used.

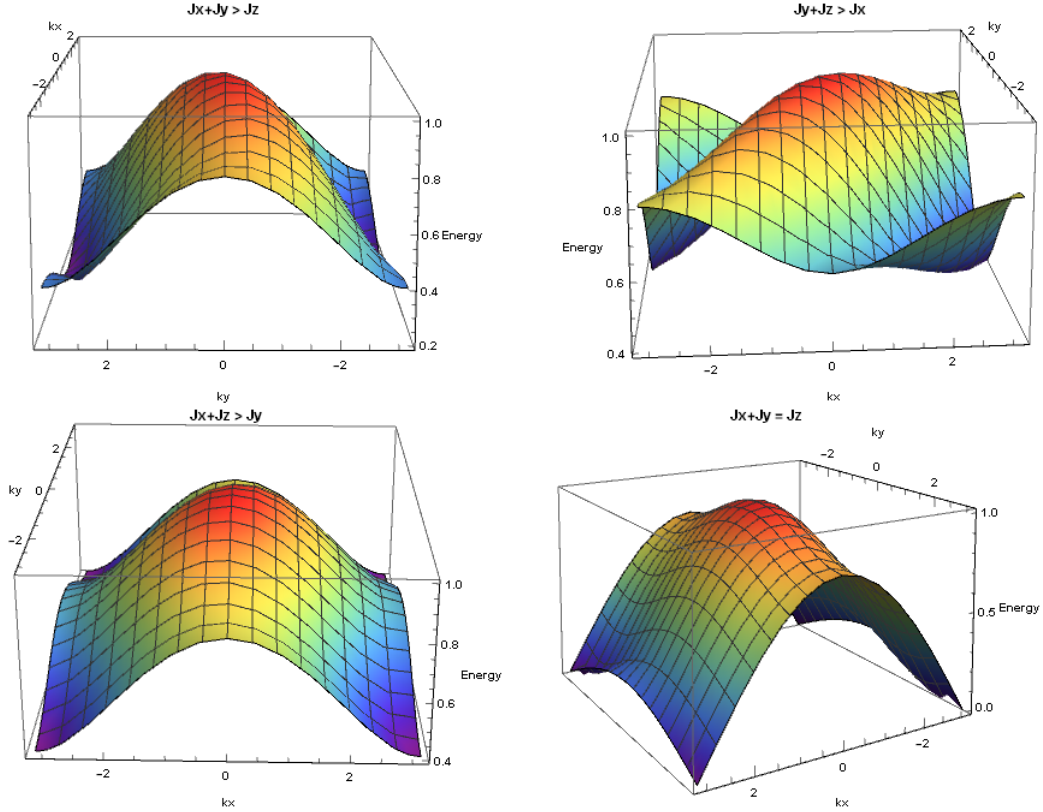


Figure 2.3: **(2.3a)** A_x gapped phase for $J_x, J_y, J_z = 0.6, 0.1, 0.3$ respectively. **(2.3b)** A_y gapped phase for $J_x, J_y, J_z = 0.2, 0.7, 0.1$ respectively. **(2.3c)** A_z gapped phase for $J_x, J_y, J_z = 0.1, 0.2, 0.7$ respectively. **(2.3d)** boundary of the gapped and gapless phase for $J_x(0.1) + J_y(0.4) = J_z(0.5)$

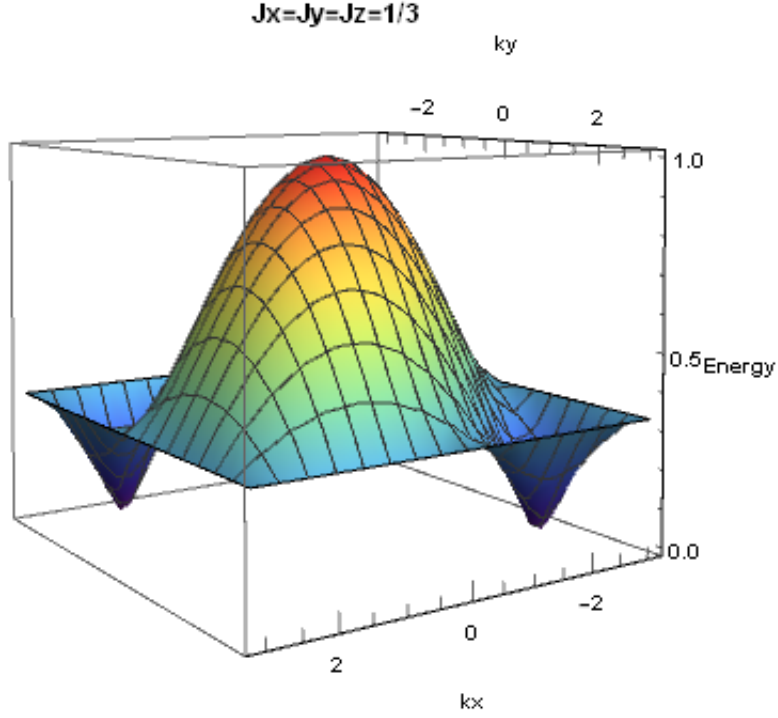


Figure 2.4: Mid point of the Phase B where energy vanishes.

The gapped phases are described by A_x , A_y and A_z where the triangle inequalities are not obeyed. The diagram for $J_x = J_y = J_z$ corresponds to the middle point of the gapless phase. The energy becomes 0 exactly at two points and those points come from the solution of equations (2.55) and (2.55).

The solutions are $k_x = \pm \arccos(-\frac{1}{2}) = \pm \frac{2\pi}{3}$ and $k_y = \pm \arccos(-\frac{1}{2}) = \pm \frac{2\pi}{3}$.

2.8 Kitaev-Heisenberg Model

After studying Kitaev model in details it is important to realize in what kind of real systems we can observe this type of specific bond directional interaction. It is really strange to have bond directional interaction in the system. However, recently people have shown the existence of Kitaev like interaction in real materials like Iridates[7]. Kitaev like interaction will give rise to the spin liquid ground state which is disordered. But introducing Heisenberg type spin interaction in presence of Kitaev type interaction in the Hamiltonian will take the system to some ordered ground state away from the Kitaev limit. So, it is in this sense Kitaev like interaction can be realised in presence of Heisenberg exchange interaction term.

2.9 KH Hamiltonian and its Phase Diagram

The Kitaev-Heisenberg[11] Hamiltonian can be written formally as the following:

$$H = (1 - \alpha) \sum_{i,j} \vec{\sigma}_i \cdot \vec{\sigma}_j - 2\alpha \sum_{\langle i,j \rangle, \gamma} \sigma_i^\gamma \sigma_j^\gamma \quad (2.63)$$

where σ are the Pauli spin 1/2 matrices and $\gamma = x, y, z$ bonds. α is the parametrised exchange coupling constant which has the value between 0 to 1. The Heisenberg coupling term is anti-ferromagnetic and Kitaev coupling term is ferromagnetic in nature. For $\alpha = 1$ we will recover the spin liquid as ground state. However, if we go away from this limit, at $\alpha = 0.5$ a phase called stripy anti-ferromagnetic ground state appears[5]. At $\alpha = 0$ it is expected that we will obtain conventional anti-ferromagnet as Kitaev term vanishes. However, very recently people have explored the full parameter space by generalising the previous Hamiltonian. In full parameter space Kitaev-Heisenberg Hamiltonian[6] will be written as:

$$H_{ij}^\gamma = A \cos \phi \sum_{\langle ij \rangle} (\vec{S}_i \cdot \vec{S}_j) + 2A \sin \phi \sum_{\gamma} S_i^\gamma S_j^\gamma \quad (2.64)$$

where $A = \sqrt{K^2 + J^2}$. K, J are corresponding Kitaev and Heisenberg exchange constants. $K = A \sin \phi$ and $J = A \cos \phi$. The angle ϕ can vary from 0 to 2π .

In full parameter space the phase diagram of Kitaev-Heisenberg model is following:

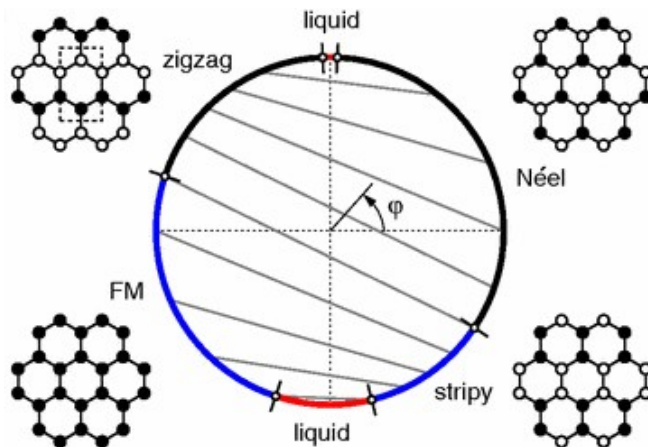


Figure 2.5: Phase diagram of KH model[6].

Fig (2.5) there are six phases present. Four of them are ordered and two of them are spin liquids. Black dots correspond to spin up direction and white dots correspond to spin down direction.

Emergence of four ordered states in KH model is very exciting. This motivates people to realise Kitaev like interaction on honeycomb magnet in presence of Heisenberg coupling. Very recently, Kitaev like spin liquid behaviour has been observed experimentally in $\alpha - RuCl_3$ [10]. Here, spins of magnetic ruthenium ions form a two dimensional hexagonal frustrated spin system structure. Existence of four ordered states in KH model have also been confirmed analytically using series expansions[8]. Finite temperature phase diagram of KH model has been explored on honeycomb lattice using functional renormalisation group method[15]. In the next chapter, we will focus on classical KH model using CMC simulation.

Chapter 3

Results and Discussion

In this chapter, we will take up the classical version of KH model and calculate some of the physical thermodynamical quantities using CMC simulation. In doing the simulation, standard Metropolis algorithm has been implemented.

3.1 Classical KH Hamiltonian

As we are discussing the classical KH model, we will consider the spins as three dimensional vectors of unit magnitude i.e. $S_x^2 + S_y^2 + S_z^2 = 1$. The Hamiltonian[12] for classical KH model is the following:

$$H = (1 - \alpha) \sum_{\langle i,j \rangle} \vec{S}_i \cdot \vec{S}_j - 2\alpha \sum_{\langle i,j \rangle \gamma} S_i^\gamma S_j^\gamma \quad (3.1)$$

where the parameter α varies between 0 and 1. The Hamiltonian has anti-ferromagnetic Heisenberg spin coupling and ferromagnetic Kitaev spin coupling. I will use this Hamiltonian for calculating various thermodynamical quantities. For $\alpha = 0$ the system will be an Heisenberg anti-ferromagnet and for $\alpha = 1$ the system will be Kitaev spin liquid.

3.2 Metropolis Algorithm

Monte-Carlo is a very good stochastic method to calculate thermodynamical quantities. Any sample spin configuration is weighed by the Boltzmann factor.

The probability that any initial state S_i moves to a final state S_f is following:

$$P(S_i \rightarrow S_f) = e^{-\beta(E_f - E_i)} \quad \text{if} \quad E_f > E_i \quad (3.2)$$

$$= 1 \quad \text{if} \quad E_f \leq E_i \quad (3.3)$$

where E_i and E_f are the initial and final energy of the system respectively.

The Metropolis algorithm[23] can be implemented in a following manner:

- First, one initialises the lattice by giving a arbitrary spin configuration of the system.
- After that choose an initial site i .
- Calculate the energy difference ΔE of the system if the spin at i is given another configuration.
- Generate a random number r between 0 and 1.
- If $\exp(-\frac{\Delta E}{k_B T}) > r$ then select the new spin configuration of the system.
- Then, one needs to go the next site j and repeat the same prescription.

3.3 Thermodynamical Quantities

Using the CMC method, some of the important thermodynamical quantities have been calculated. In the thermodynamical limit, the interesting quantities are average energy, average magnetisation, specific heat. I calculated these quantities varying with temperature for classical KH model on honeycomb lattice and triangular lattice.

$$C_v = N^2 \frac{\langle E^2 \rangle - \langle E \rangle^2}{T^2} \quad (3.4)$$

$$\langle M \rangle = (1/N^2) \left\langle \sqrt{\sum_i (S_i^x)^2 + \sum_i (S_i^y)^2 + \sum_i (S_i^z)^2} \right\rangle \quad (3.5)$$

3.4 MC results on honeycomb lattice

We have carried out the CMC simulation on classical KH model on honeycomb lattice. We have explored how thermodynamical quantities like specific heat, magnetisation,

energy change with temperature. We have calculated the following quantities on 14×14 lattice size. While running the simulations, the following parameters were used:

- Equilibration steps were 10000.
- Averaging steps were 10000.
- Temperature step size was 0.07 in the unit of exchange constant α .

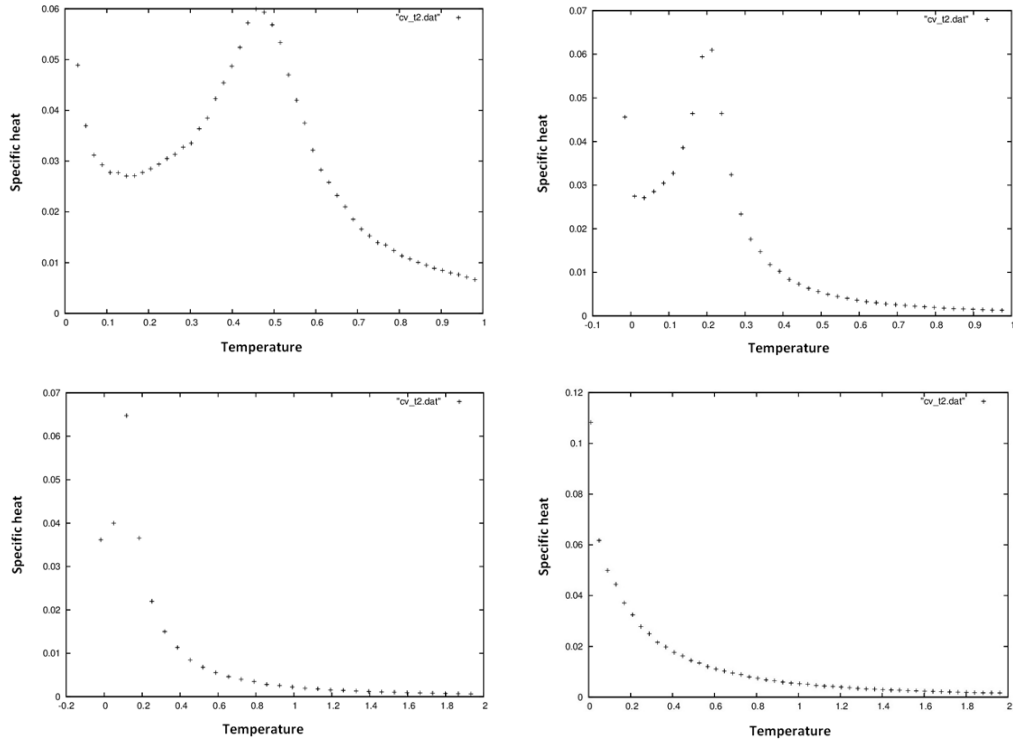


Figure 3.1: **(3.1a)** $C_v(T, \alpha = 0)$ **(3.1b)** $C_v(T, \alpha = 0.5)$ **(3.1c)** $C_v(T, \alpha = 0.75)$
(3.1d) $C_v(T, \alpha = 1)$

From the above figures we see how the specific heat changes with temperature for various values of α . It is interesting to see that when we are approaching the Heisenberg limit (α tending towards 0), there is a clear indication of phase transition as the specific heat curves start getting a peak.

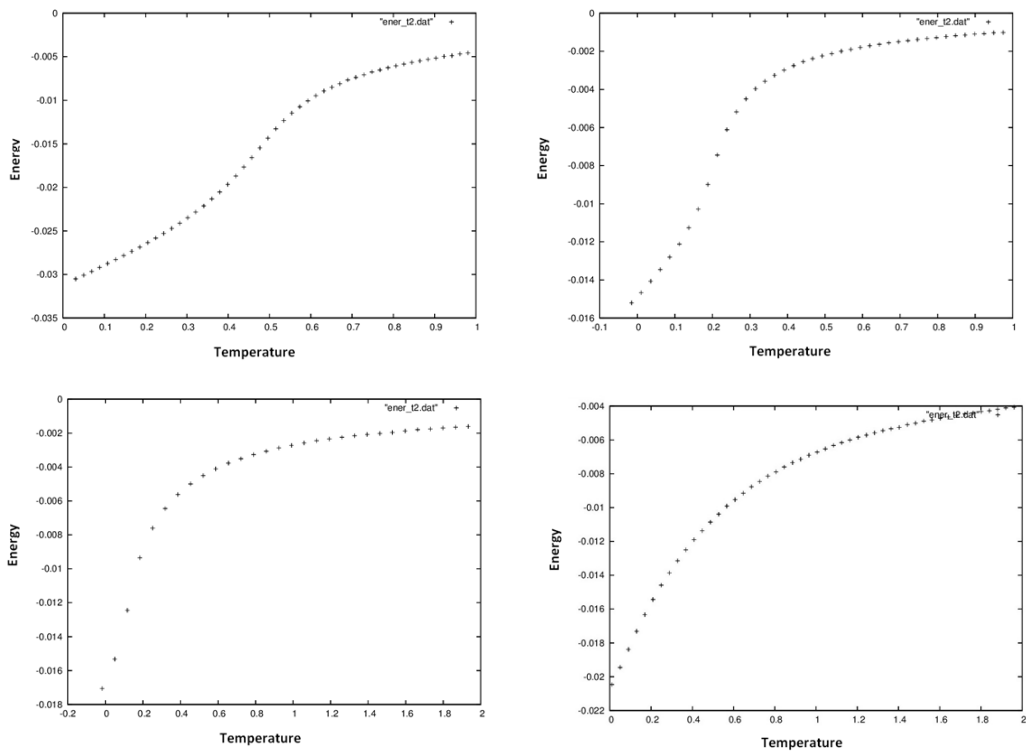


Figure 3.2: **(3.2a)** $E(T, \alpha = 0)$ **(3.2b)** $E(T, \alpha = 0.5)$ **(3.2c)** $E(T, \alpha = 0.75)$
(3.2d) $E(T, \alpha = 1)$

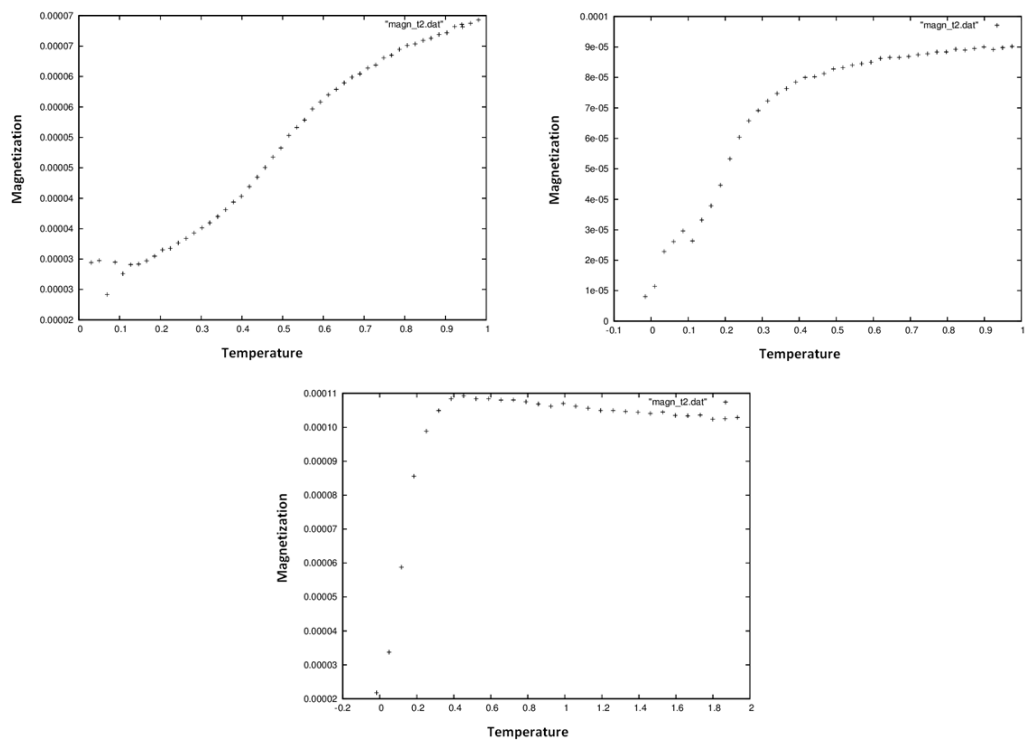


Figure 3.3: **(3.3a)** $M(T, \alpha = 0)$ **(3.3b)** $M(T, \alpha = 0.5)$ **(3.3c)** $M(T, \alpha = 1)$

3.5 MC results on triangular lattice

We have also investigated the variation of specific heat, magnetisation and energy with temperature on triangular lattice. In this case, the system size taken was 60×60 . While running the simulations, the following parameters were used:

- Equilibration steps were 20000.
- Averaging steps were 20000.
- Temperature step size was 0.026 in the unit of exchange constant α .

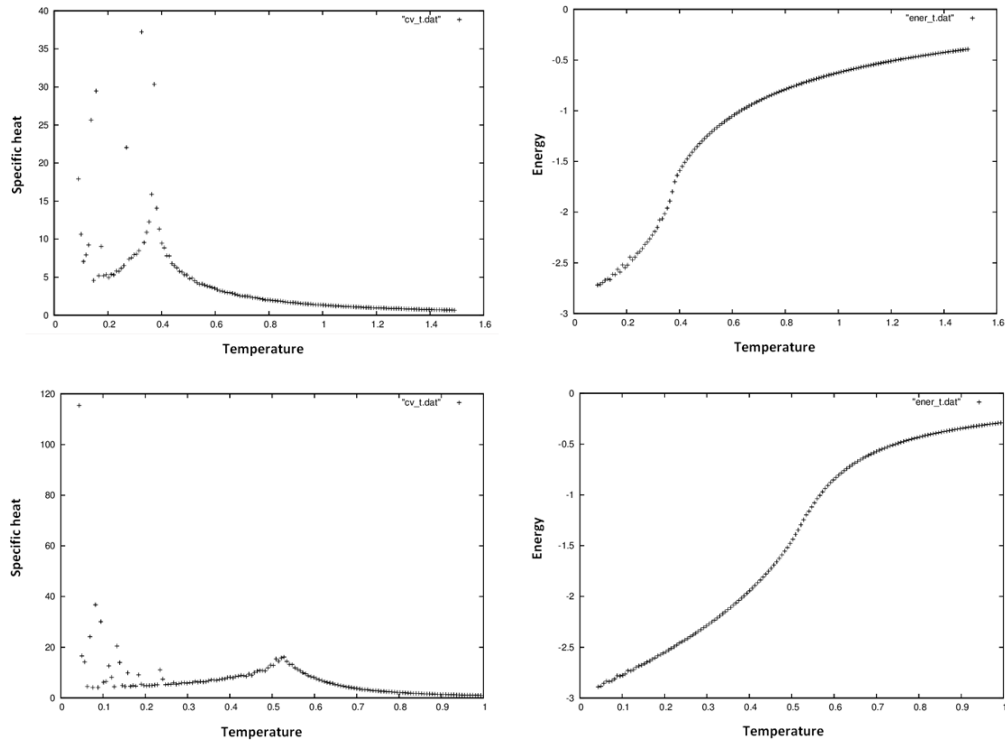


Figure 3.4: **(3.4a)** $C_v(T, \alpha = 0)$ **(3.4c)** $C_v(T, \alpha = 0.5)$ **(3.4b)** $E(T, \alpha = 0)$
(3.4d) $E(T, \alpha = 0.5)$

In the above figures, we see that the system always goes to some ordered state when we approach to the low temperature for various α values.

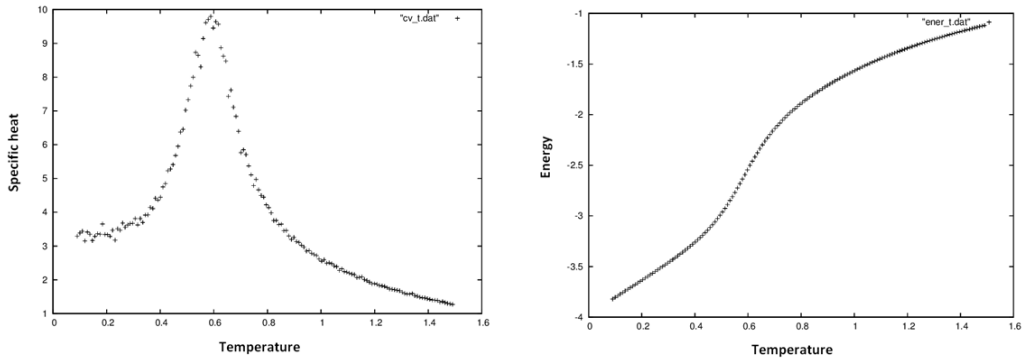


Figure 3.5: (3.4e) $C_v(T, \alpha = 1)$ (3.4f) $E(T, \alpha = 1)$

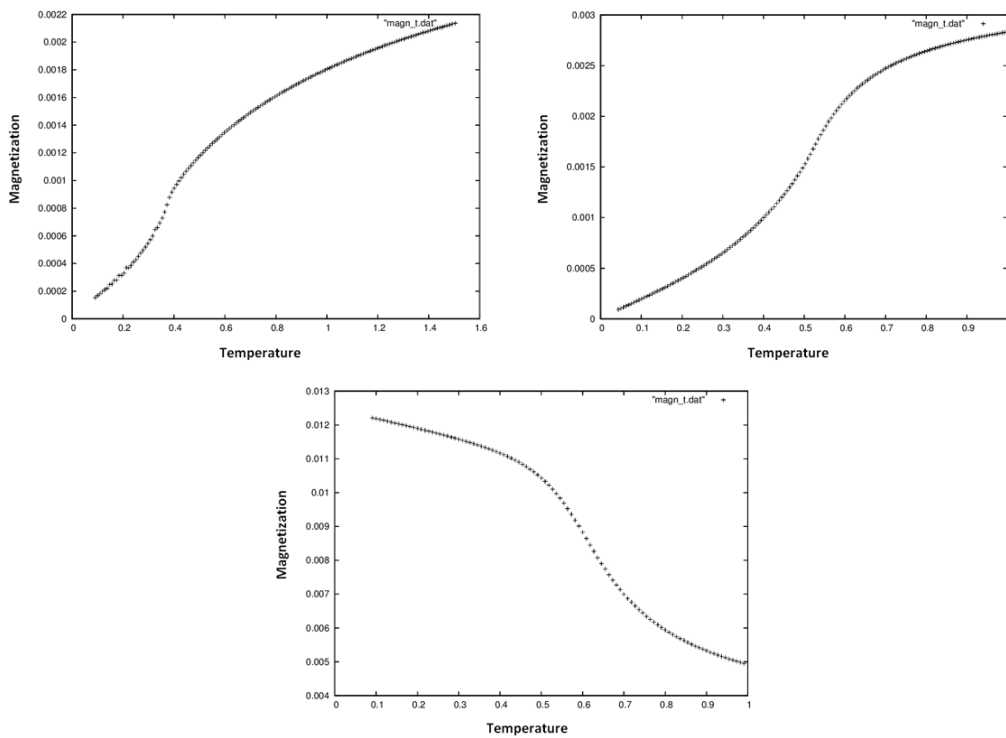


Figure 3.6: (3.6a) $M(T, \alpha = 0)$ (3.6b) $M(T, \alpha = 0.5)$ (3.6c) $M(T, \alpha = 1)$

3.6 Structure Factor

We also calculate structure factors for triangular lattice in order to find the magnetic ordering of ground states at two extreme limit of α namely for $\alpha = 1$ and $\alpha = 0$. The structure factor formula can be written as following:

$$S_{\vec{k}} = \frac{1}{N^2} \sum_{\langle ij \rangle} (\vec{S}_i \cdot \vec{S}_j) e^{i\vec{k}(\vec{r}_i - \vec{r}_j)} \quad (3.6)$$

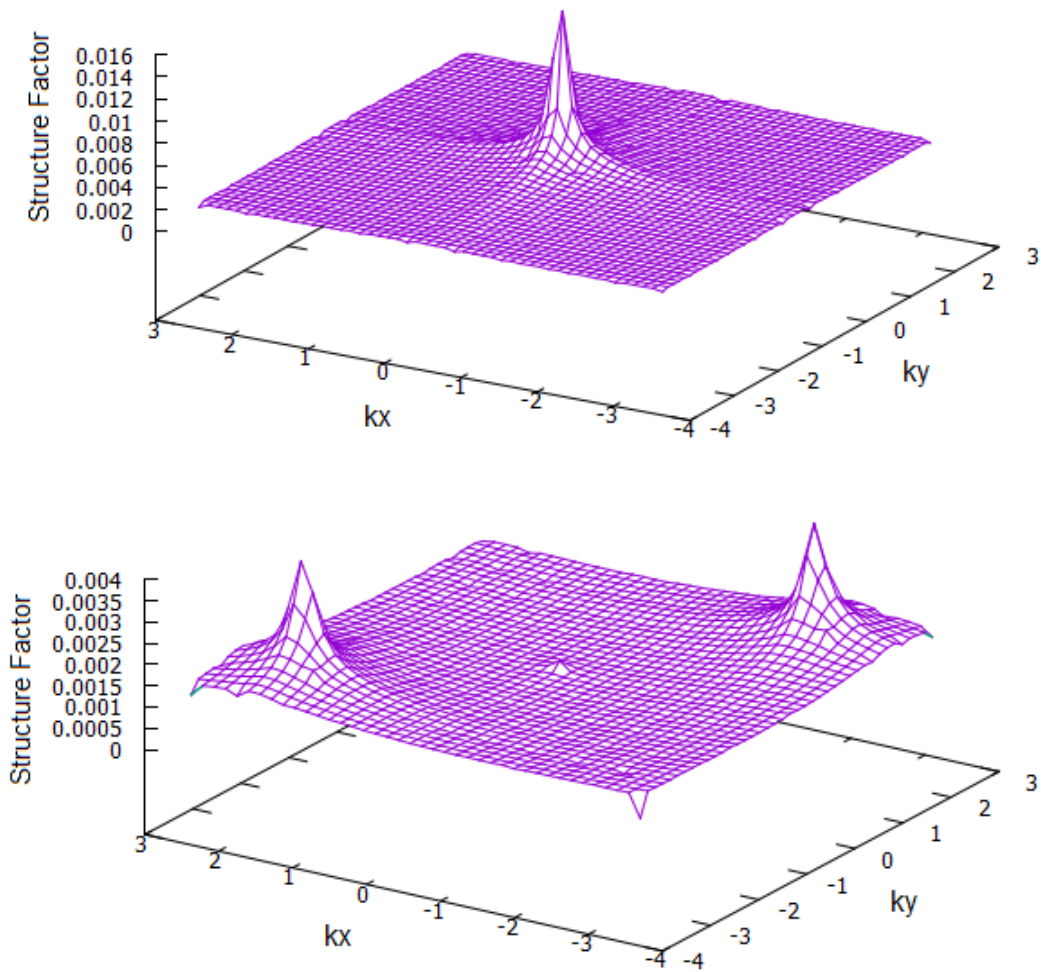


Figure 3.7: **(3.7a)** Structure factor for $\alpha = 1$ on 30×30 triangular lattice. **(3.7b)** Structure factor for $\alpha = 0$ on 30×30 triangular lattice.

For $\alpha = 1$, there appears one peak in the structure factor plot corresponding to the ferromagnetic ground state. Whereas for $\alpha = 0$ the system shows the signature of a neel type anti-ferromagnetic ground state.

3.7 Conclusion

- After calculating several thermodynamical quantities using CMC method, we have shown that in the classical KH model on honeycomb lattice there do exist a spin liquid state for $\alpha = 1$. We come to this conclusion based on the specific heat, energy and magnetisation curves. As we change α from 1 and go towards 0, at low temperature long range ordered state starts appearing. And hence we can observe significant changes in the specific heat, energy and magnetisation plots. Even though Mermin-Wagner theorem[18] states that we cannot have long range ordered state in two dimension or below at finite temperature, here the ordered state is emerging due to order by disorder mechanism[9]. The clear peaks appearing in specific heat plots away from Kitaev limit indicate the phase transition. So, the existence of spin liquid in Kitaev limit and phase transition away from the Kitaev limit is observed.
- On honeycomb lattice for $\alpha = 0$ the anti-ferromagnetic state is observed from the magnetisation graphs as expected. Because $\alpha = 0$ means Kitaev term vanishes and the Heisenberg term remains. So, the system prefers anti-ferromagnetic ordering as the exchange constant value is positive.
- We have carried out CMC simulations on triangular lattice also. However, in this case, we have not found any existence of spin liquid behaviour for $\alpha = 1$. Rather, we observe phase transition taking place for various ranges of α at different temperature. So, CMC simulation is not able to give any trace of spin liquid states on triangular lattice for classical KH model.
- From the structure factor calculation on triangular lattice we can see that there exist ferromagnetic ground state for $\alpha = 1$ and anti-ferromagnetic ground state for $\alpha = 0$.

3.8 Future Outlook

- It will be interesting to study Majorana fermions of the spin 1/2 Kitaev Hamiltonian (2.32) in presence of constant background fields numerically. For each configuration of static background gauge field, one can diagonalise the quadratic Majorana fermionic Hamiltonian. So the energy spectrum can be obtained and density of states for itinerant Majorana fermions can also be plotted. In relation to that, transport property like optical conductivity can give information about metallic behaviour of Majorana fermions. One may also calculate thermodynamical quantities[20] like specific heat, entropy.
- One can use CMFT method to understand the dynamics of Majorana fermions. In CMFT, lattice sites are divided into clusters in such a way that equivalence of all sites is preserved in a cluster[25]. Here interaction between clusters are treated on a mean field level.
- Spin-spin correlation can give information about the orderedness of the system. So, it will be interesting to calculate spin-spin correlation function using CMFT.

Appendix A

Anti-Commutation Relation

$$\begin{aligned}\{\sigma^x, \sigma^y\} &= \sigma^x \sigma^y + \sigma^y \sigma^x \\ &= iC^x C iC^y C + iC^y C iC^x C \\ &= -C^x C C^y C - C^y C C^x C \\ &= +C^x C^y C^2 + C^y C^x C^2 \\ &= C^x C^y + C^y C^x && \text{using } C^2 = 1 \\ &= C^x C^y - C^x C^y && \text{using } \{C^x, C^y\} = 0 \\ &= 0\end{aligned}$$

$$\begin{aligned}\{\sigma^x, \sigma^x\} &= 2(\sigma^x)^2 \\ &= 2i^2 C^x C C^x C \\ &= -2C^x C C^x C \\ &= +2(C^x)^2 C^2 && \text{using } \{C^x, C\} = 0 \\ &= 2 && \text{using } (C^x)^2 = 1 \text{ and } C^2 = 1\end{aligned}$$

Hence,

$$\{\sigma^\alpha, \sigma^\beta\} = 2\delta_{\alpha\beta} \quad \text{where } \alpha, \beta = x, y, z \quad (\text{A.1})$$

$$\begin{aligned}
\hat{D} &= C^x C^y C^z C \\
&= C^x C C^y C^z \\
&= \frac{1}{i}(C_1 - C_1^\dagger)(C_1 + C_1^\dagger)(C_2 + C_2^\dagger)\frac{1}{i}(C_2 - C_2^\dagger) \\
&= -1(C_1 - C_1^\dagger)(C_1 + C_1^\dagger)(C_2 + C_2^\dagger)(C_2 - C_2^\dagger) \\
&= (C_1^\dagger - C_1)(C_1 + C_1^\dagger)(C_2 + C_2^\dagger)(C_2 - C_2^\dagger) \\
&= \left(C_1^\dagger C_1 + (C_1^\dagger)^2 - (C_1)^2 - C_1 C_1^\dagger \right) \left((C_2)^2 - C_2 C_2^\dagger + C_2^\dagger C_2 - (C_2^\dagger)^2 \right) \\
&= \left(C_1^\dagger C_1 - C_1 C_1^\dagger \right) \left(C_2^\dagger C_2 - C_2 C_2^\dagger \right) \quad \text{using} \quad (C_1)^2, (C_1^\dagger)^2, (C_2)^2, (C_2^\dagger)^2 = 0 \\
&= \left(C_1^\dagger C_1 - (1 - C_1^\dagger C_1) \right) \left(C_2^\dagger C_2 - (1 - C_2^\dagger C_2) \right) \\
&= (2C_1^\dagger C_1 - 1)(2C_2^\dagger C_2 - 1) \tag{A.2}
\end{aligned}$$

Bibliography

- [1] Alexei Kitaev, *Annals of Physics* **321**, (2006)
- [2] Leon Balents, *Nature* **464**, 199-208, (2010)
- [3] Young S. Lee et.al, *Nature* **492**, 406-410, (2012)
- [4] Saptarshi Mandal and Naveen Surendran, *Phys. Rev. B* **79**, 024426, (2009)
- [5] J. Chaloupka, G. Jackeli, G. Khaliulin, *Phys. Rev. Lett.* **105**, 027204, (2010)
- [6] J. Chaloupka, G. Jackeli, G.Khaliulin, *Phys. Rev. Lett.* **110**, 097204, (2013)
- [7] B.J.Kim et.al, *Nature Physics* **11**, 462466, (2015)
- [8] J Oitmaa, *Phys. Rev. B* **92**, 020405(R), (2015)
- [9] Craig Price and Natalia B. Perkins, *Phys. Rev. B* **88**, 024410, (2013)
- [10] A. Banerjee et.al, *nature materials* **10.1038/nmat4604**, (2016)
- [11] Yogesh Singh et.al, *Phys. Rev. Lett.* **108**, 127203, (2012)
- [12] Craig C. Price and Natalia B. Perkins, *Phys. Rev. Lett.* **109**, 187201, (2012)
- [13] Fa Wang, *Phys. Rev. B* **82**, 024419, (2010)
- [14] Xiao-Gang Wen, *Phys. Rev. B* **65**, 165113, (2002)
- [15] Johannes Reuther, Ronny Thomale, Simon Trebst, *Phys. Rev. B* **84**, 100406(R), (2011)
- [16] Yi Zhou, Kazushi Kanoda, Tai-Kai Ng, *arXiv* **1607.03228v2**, (2016)
- [17] Simon Trebst, *arXiv* **1701.07056v1**, (2017)

- [18] N. D. Mermin and H. Wagner, *Phys. Rev. Lett.* **17**, 1133, (1966)
- [19] Andrei Catuneanu, Jeffrey G. Rau, Heung-Sik Kim, and Hae-Young Kee, *Phys. Rev. B* **92**, 165108, (2015)
- [20] Joji Nasu, Masafumi Udagawa, and Yukitoshi Motome, *Phys. Rev. B* **92**, 115122, (2015)
- [21] E. Lieb, *Phys. Rev. Lett.* **73**, 2158, (1994)
- [22] Saptarshi Mandal, Investigations on the Kitaev Model and some of its generalisations, 2011.
- [23] David P. Landau and Kurt Binder, A Guide to Monte Carlo Simulations in Statistical Physics. Second Edition. Cambridge University Press, 2005.
- [24] Han-Dong Chen and Zohar Nussinov, *Journal of Physics A: Mathematical and Theoretical* **41**, 7, (2008)
- [25] Daisuke Yamamoto, *Phys. Rev. B* **79**, 144427, (2009)
- [26] sciencedaily.com